# Analysis of the Input-Output Couplings in a Wastewater Treatment Plant Model

Pär Samuelsson, Björn Halvarsson and Bengt Carlsson

Division of Systems and Control, Department of Information Technology, Uppsala University,
P O Box 337, SE–751 05, Uppsala, Sweden
E-mail: Par.Samuelsson@it.uu.se, Bjorn.Halvarsson@it.uu.se, Bengt.Carlsson@it.uu.se

**Abstract**

This paper considers the problem of channel interaction in multivariable systems. As an application, nitrate removal in the activated sludge process in a wastewater treatment plant is studied. To evaluate the degree of channel interaction, two different tools are compared; the well known Relative Gain Array (RGA) and the more recently developed Hankel Interaction Index Array (HIIA). The results of the analysis are discussed from a process knowledge point of view, and are also illustrated with some control experiments. The main conclusion is that both the analysis tools provide reasonable results in this case. The HIIA, however, gives a deeper insight about the actual cross couplings in the system. This insight may also be used in order to design suitable structured multivariable controllers.

# 1 Introduction

A common problem in the area of multivariable control is channel interaction, i.e. when one input signal affects several output signals. This problem occurs in several common application fields in multivariable process control, for example in wastewater treatment. In the process industry, a complexity of several hundred control loops is not uncommon for a system, see Wittenmark *et al.* (1995). The great number of input and output signals may of course give rise to interactions in certain loops. If the interactions are not too large, it might be sufficient to use a number of single input single output control loops in order to control the system, so called decentralised control. An important question that rises is then the so called pairing problem: *Which input signal should be selected to control which output signal to get the most efficient control with a low degree of interaction?* If the interactions in the open loop system are severe, however, a multivariable control structure may be preferable. An interesting problem is then how to choose this control structure. If a sparse control structure can be used instead of a full multivariable one, much could be gained in terms of reducing the controller complexity.

Over the years, several different measures for quantifying the level of input-output interactions in a system have been developed. Among the first, and to this day probably most commonly used, was the Relative Gain Array (RGA) introduced by Bristol (1966). Originally, the RGA considered only the stationary properties of the plant, but a dynamic extension was proposed later, see Kinnaert (1995) for a survey. Many other different modifications of the RGA have been proposed since it was introduced, examples of later refinements can be found in, for instance, Häggblom (1997), Schmidt and Jacobsen (2003) and Mc Avoy *et al.* (2003). The RGA is a measure that can be used in order to decide a suitable input-output pairing when a decentralised control structure is to be used, and also to decide whether a certain pairing should be avoided. This measure, however, often provides limited knowledge about when to use multivariable controllers and gives no indication of how to choose multivariable controller structures.

Relatively recently, a different approach for investigating channel interaction was introduced by Conley and Salgado (2000). In this approach the controllability and observability Gramians of a system are used in order to quantify the degree of interaction. This work was further developed in the paper Wittenmark and Salgado (2002) where the Hankel norm of the system was used to develop the so called Hankel Interaction Index Array (HIIA).

Compared to the RGA, there are some major differences. When using the HIIA, the whole frequency range is taken into account, not only the stationary case. Another difference is that the RGA assumes a decentralised control structure to be used, and therefore attempts to suggest the best possible input-output pairing. This is not the case with the HIIA, that rather considers the controllability and the observability of every sub-system in the plant. This measure may therefore be valuable when evaluating alternatives to decentralised control structures. In Conley and Salgado (2000), it is also shown how to do this, even though it is not clearly stated in Wittenmark and Salgado (2002). There are also cases, see Chien *et al.* (1992) and Kinnaert (1995), where the RGA fails to suggest a proper pairing due to large off-diagonal elements or triangular structure in the plant. This is also pointed out in Birk (2002) and Halvarsson (2003). On the other hand, a major drawback of the HIIA compared to the RGA is that it is scaling dependent. It is therefore of great importance that the system has been scaled in a physically relevant way in order for the HIIA to provide meaningful results.

In this paper, both the RGA and the HIIA are calculated for different operating points of a certain process in a bioreactor model. Cross couplings in other processes in such systems have previously been studied by Ingildsen (2002) and Halvarsson (2003). The bioreactor model studied here is a pre-denitrifying wastewater treatment plant. The results of the methods are compared and discussed. The aim is to illustrate the different conclusions that can be drawn, and also to discuss the results from a process knowledge point of view.

The layout of this paper is as follows: In Section 2, some basics of the RGA is described. Further, the HIIA is described in Section 3. The bioreactor model used to illustrate the RGA and HIIA methods is found in Section 4, and the presented model is analyzed with respect to the RGA and the HIIA in Section 5. To illustrate the results of the analysis in Section 5, some control experiments are performed in Section 6. In Section 7, the results of Sections 5 and 6 are discussed. The general conclusions are presented in Section 8.

# 2 The Relative Gain Array (RGA)

## 2.1 Definition

The static RGA for a quadratic plant is given by

$$\mathrm{RGA}(G(0)) = G(0). * (G(0)^{-1})^T \tag{1}$$

where G(0) is the steady-state transfer function matrix and ".∗" denotes the Hadamard or Schur product (i.e. elementwise multiplication). Each element in the RGA can be regarded as the quotient between the open-loop gain and the closed-loop gain. Hence, the RGA element $(i, j)$ is the quotient between the gain in the loop between input $j$ and output $i$ when all other loops are open and the gain in the same loop when all other loops are closed. For a more complete discussion of the RGA, see e.g. Bristol (1966), Kinnaert (1995) or Skogestad and Postlethwaite (1996).

The definition of the dynamic RGA is basically the same as for the original RGA, except that now the plant gain, $G$, is allowed to be measured at any frequency $\omega$. Not surprisingly, this dynamic version of the RGA possesses the same properties as the steady-state RGA. Still, each frequency point has to be considered separately

$$\mathrm{RGA}(G(i\omega)) = G(i\omega). * (G(i\omega)^{-1})^T. \tag{2}$$

Later in this paper, only the static RGA is used. This can be motivated by the slow time constants in the considered bioreactor system.

## 2.2 Pairing Recommendation

In the case of a 2×2 system, a symmetric RGA matrix is obtained:

$$\mathrm{RGA}(G(0)) = \begin{bmatrix} \lambda & 1-\lambda \\ 1-\lambda & \lambda \end{bmatrix} \tag{3}$$

Depending on the value of $\lambda$, five different cases occur (Kinnaert 1995):

$\lambda = 1$**:** This is the ideal case when no interaction between the loops is present. The pairing should be along the diagonal, i.e. $u_1 - y_1$ and $u_2 - y_2$;

$\lambda = 0$**:** This is the same situation as above, except that now the suggested pairing is along the anti-diagonal, i.e. $u_1 - y_2$, $u_2 - y_1$;

$0 < \lambda < 1$**:** This case indicates that the gain increases when the loops are closed, thus there is interaction;

$\lambda > 1$**:** Now, the gain decreases when the loops are closed. This situation is therefore also undesirable;

$\lambda < 0$**:** This situation corresponds to the worst case scenario since now even the sign changes when the loops are closed and this is highly undesirable.

The conclusion is that $u_1$ should only be paired with $y_1$ when $\lambda > 0.5$. The closer $\lambda$ is to one, the more likely is this configuration to work, that is, the less is the interaction in the system. For all other values of $\lambda$, $u_1$ should be paired with $y_2$. For the higher-dimensional case, the rule should be to choose pairings that corresponds to an RGA element close to one. Negative pairings should definitely be avoided.

# 3 Gramian-based Interaction Measures

As mentioned in the introduction, the RGA suffers from some important disadvantages, such as its inability to deal properly with triangular plants, and its limitation to consider each frequency separately. Conley and Salgado (2000) proposed a new interaction measure based on Gramians able to handle both of the above-mentioned pitfalls. Recently, a modified version of the interaction measure was suggested by Wittenmark and Salgado (2002) where the Hankel norm is used. This measure is also suitable for designing structured multivariable controllers.

Consider a linear system, with inputs given by the $n \times 1$ vector $u(t)$ and outputs given by $y(t)$. Given the state vector $x(t)$, the system can be described as a state space realisation

$$\begin{aligned} \dot{x}(t) &= Ax(t) + Bu(t) \\ y(t) &= Cx(t) + Du(t) \end{aligned} \tag{4}$$

where $A$, $B$, $C$ and $D$ are real matrices of dimension $n \times n$, $n \times m$, $p \times n$ and $p \times m$, respectively. Then, the controllability Gramian, $\Gamma_c$, and the observability Gramian, $\Gamma_o$, for the system given in (4) are defined as

$$\Gamma_c = \int_0^\infty e^{A\tau} B B^T e^{A^T \tau} \mathrm{d}\tau \tag{5}$$

$$\Gamma_o = \int_0^\infty e^{A^T \tau} C^T C e^{A\tau} \mathrm{d}\tau. \tag{6}$$

These are measures of how hard it is to observe and to control the states of the given system. As shown by Conley and Salgado (2000) and Wittenmark and Salgado (2002), it is possible to split the system given by $(A, B, C, D)$ into fundamental subsystems $(A, B_j, C_i, D_{ij})$ where $B_j$ is the $j$:th column in $B$, $C_i$ is the $i$:th row in $C$ and $D_{ij}$ is the $(i, j)$:th element of $D$. Then for each of these, the controllability and the observability Gramian can be calculated. The controllability and observability Gramians for the full system will then

be the sum of the Gramians for all the subsystems.

Unfortunately, both the controllability and the observability Gramian will depend on the chosen state space realisation. However, the eigenvalues of the product of these will not.

## 3.1 The Hankel Interaction Index Array (HIIA)

The Hankel norm for a system with transfer function $G(s)$ is defined as

$$\|G(s)\|_H = \sqrt{\lambda_{max}(\Gamma_c \Gamma_o)} = \sigma_1^H \tag{7}$$

where $\sigma_1^H$ is the maximum Hankel singular value. Hence, this measure is invariant with respect to the state space realization and it is therefore well suited as a combined measure for controllability and observability. In Wittenmark and Salgado (2002) it is shown that the Hankel norm of $G(s)$ given in (7) can also be interpreted as a gain between past inputs and future outputs. Then, if the Hankel norm is calculated for each fundamental subsystem and arranged in a matrix $\Sigma_H$ given by

$$[\Sigma_H]_{ij} = \|G_{ij}(s)\|_H \tag{8}$$

this matrix can be used as an interaction measure. In Wittenmark and Salgado (2002) a normalised version, the Hankel Interaction Index Array (HIIA), is proposed:

$$[\Sigma_H]_{ij} = \frac{\|G_{ij}(s)\|_H}{\Sigma_{kl}\|G_{kl}(s)\|_H} \tag{9}$$

In the HIIA, the larger the element, the larger the impact of the corresponding input signal on the specific output signal. Even though not directly stated by Wittenmark and Salgado (2002), expected performance for different control structures can certainly be compared by summing the elements in $\Sigma_H$: Clearly, due to the normalisation, the aim is to find the simplest control structure that gives a sum as near one as possible. In the slightly different interaction measure proposed by Conley and Salgado (2000) this is used. If decentralised control is to be used, the pairing rule will be the same as for the RGA, i.e. for each row (i.e. output) select the largest element.

When $G_{ij} = 0$ the Gramian product, $\Gamma_c^{(j)}\Gamma_o^{(i)}$, will be zero and so will the corresponding element in the matrix $\Sigma_H$. This implies that the structure of $\Sigma_H$ will be the same as the structure of $G$ and thus, non-diagonal elements will not be hidden as in the case of the RGA. This motivates further that

the HIIA can also be used to evaluate other control structures than just the decentralised ones.

As shown in examples given by Wittenmark and Salgado (2002), the HIIA outperforms the RGA when dealing with systems that have interactions with non-monotonic frequency behaviour. The reason for this is that the full dynamics of the system will be taken into account when using Gramians. If the objective is to study the interactions in a specific frequency range only, then the original system can be filtered before the HIIA is calculated, see Wittenmark and Salgado (2002).

# 4 The Bioreactor Model

In this paper, the RGA and the HIIA will be used on a bioreactor model describing the denitrification process (conversion of nitrate to nitrous oxide). Generally, the bioreactor is connected to a clarifier, and the process consisting of these two parts is commonly called an activated sludge process (ASP), see Henze *et al.* (1995). In recent years, the control problems in this area have become more and more important due to increased demands on the effluent water quality, see for instance Olsson and Newell (1999), Vanrolleghem and Gillot (2002), Ingildsen *et al.* (2002), Yuan *et al.* (2002) and Jeppsson *et al.* (2001). In an ASP configured for nitrogen removal, ammonium is oxidized to nitrate under aerobic conditions. This process is called *nitrification*. The nitrate formed by the nitrification process, in turn, is converted into gaseous nitrogen under anoxic conditions, this is the so called denitrification. Therefore, a multi-step configuration is generally needed in order to perform an efficient nitrogen removal. If the anoxic part of the process is placed before the aerobic, the process is said to be pre-denitrifying.

For the denitrification process to take place, a sufficient amount of organic substrate (readily biodegradable organic substrate) is needed as well as anoxic conditions, i.e. absence of dissolved oxygen. In a pre-denitrifying system, the access to nitrate in the anoxic part is achieved by recirculating nitrate rich water from the aerobic to the anoxic part of the plant. To ensure that enough readily biodegradable substrate is present, an external carbon source (for example ethanol) is often added to the anoxic part. It is thus natural to consider the flow rates of the internal recirculation and the addition of an external carbon source as control signals (manipulated variables) in the denitrification process, although we will here use the concentration of readily biodegradable organic substrate in the influent water as an input instead of

an external carbon source. A natural selection of output signals (controlled variables) is the nitrate levels in the anoxic and the aerobic (effluent) compartments respectively. Several papers in the literature deal with the above described control problem, see for instance Carlsson and Rehnström (2002).

The probably most used mathematical model describing biological nitrogen removal is the IAWQ Activated Sludge Model No. 1 (ASM1), see Henze *et al.* (1987) for a full description. This is a rather complex nonlinear model including eight different processes:

- $P_1$ Aerobic growth of heterotrophs;
- $P_2$ Anoxic growth of heterotrophs;
- $P_3$ Aerobic growth of autotrophs;
- $P_4$ Decay of heterotrophs;
- $P_5$ Decay of autotrophs;
- $P_6$ Ammonification;
- $P_7$ Hydrolysis of entrapped organic materials;
- $P_8$ Hydrolysis of entrapped organic nitrogen.

Further, thirteen state variables given as concentrations of different compounds are used in the model (all have the unit mg/l):

- $S_I$ Soluble inert organic matter;
- $S_S$ Soluble readily biodegradable substrate;
- $X_I$ Particulate inert organic matter;
- $X_S$ Slowly biodegradable substrate;
- $X_{B,A}$ Active autotrophic biomass;
- $X_{B,H}$ Active heterotrophic biomass;
- $X_P$ Particulate products arising from biomass decay;
- $S_O$ Dissolved oxygen;
- $S_{NO}$ Soluble nitrate nitrogen;

- $S_{NH}$ Soluble ammonium nitrogen;
- $S_{ND}$ Soluble biodegradable organic nitrogen;
- $X_{ND}$ Particulate biodegradable organic nitrogen;
- $S_{ALK}$ Alkalinity.

Due to this complexity, the model is not very suitable for control purposes. Instead a somewhat simplified model will be used in the analysis carried out in this paper. In the following subsection, the simplified model is presented and motivated.

## 4.1 The simplified bioreactor model

As discussed, due to its complexity, the full ASM1 model is not suitable for analysing interactions. Instead a simplified model will be used. First, a simplified nonlinear model describing the nitrate removal is discussed. The resulting model used here describes a pre denitrifying process with one anoxic and one aerobic compartment, see Figure 1. In the analysis in the next section, this model is linearised for different operating points, and the RGA and HIIA analysis is performed on the linearised models. The reduced order nonlinear model is more thoroughly discussed by Ingildsen (2002).

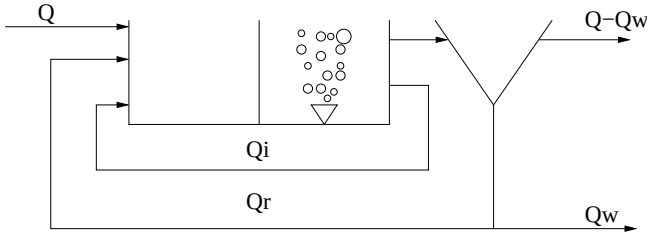


Figure 1: An ASP with one anoxic and one aerobic compartment and a clarifier. The influent flow rate is denoted $Q$, the internal recirculation flow rate $Q_i$, the flow rate of recirculated sludge $Q_r$ and the excess sludge flow rate $Q_w$.

By considering slowly changing variables in the ASM1 as constant, the number of differential equations that has to be taken into account can be fairly reduced. For a start, growth of autotrophic and heterotrophic biomass ($X_{B,A}$ and $X_{B,H}$ respectively) is slow compared to the rest of the states in the process. When the biomass is constant, so are the decay ratio of the

biomasses in ASM1, and these processes ($P_4$ and $P_5$) may be omitted since they will not contribute to the linearised model used in the analysis. In Ingildsen (2002) it is also stated that the hydrolysis processes ($P_6$ and $P_7$) and the nitrification ($P_8$) are almost constant. These processes are therefore also omitted in the simplified nonlinear model. A direct impact of this simplification is that the states $X_S$, $S_{ND}$ and $X_{ND}$ will not affect the other states and can therefore be omitted too. Further, the states $S_I$, $X_I$, $X_P$ and $S_{ALK}$ do not have any impact on the remaining states and it is thus meaningless to include these in the model. Finally, it is assumed that the dissolved oxygen concentration in the aerobic part of the process can be efficiently controlled and kept at some constant value. This makes it possible to neglect the dynamics of the dissolved oxygen in the aerobic part. Using the assumptions above, the resulting simplified nonlinear differential equation model describing one anoxic and one aerated compartment will according to Ingildsen (2002) be

$$
\begin{aligned}
\dot{S}_{NH,1} =& \frac{Q}{V_1} S_{NH,in} - \frac{Q+Q_i}{V_1} S_{NH,1} + \frac{Q_i}{V_1} S_{NH,2} - i_{XB} P_{2,1} - i_{XB} P_{1,1} - (i_{XB} + \frac{1}{Y_A}) P_{3,1} \\
\dot{S}_{NH,2} =& \frac{Q+Q_i}{V_2} S_{NH,1} - \frac{Q+Q_i}{V_2} S_{NH,2} - i_{XB} P_{2,2} - i_{XB} P_{1,2} - (i_{XB} + \frac{1}{Y_A}) P_{3,2} \\
\dot{S}_{NO,1} =& - \frac{Q+Q_i}{V_1} S_{NO,1} + \frac{Q_i}{V_1} S_{NO,2} - \frac{1-Y_H}{2.86 Y_H} P_{2,1} + \frac{1}{Y_A} P_{3,1} \\
\dot{S}_{NO,2} =& \frac{Q+Q_i}{V_2} S_{NO,1} - \frac{Q+Q_i}{V_2} S_{NO,2} - \frac{1-Y_H}{2.86 Y_H} P_{2,2} + \frac{1}{Y_A} P_{3,2} \\
\dot{S}_{S,1} =& \frac{Q}{V_1} S_{S,in} - \frac{Q+Q_i}{V_1} S_{S,1} + \frac{Q_i}{V_1} S_{S,2} - \frac{1}{Y_H} P_{2,1} - \frac{1}{Y_H} P_{1,1} \\
\dot{S}_{S,2} =& \frac{Q+Q_i}{V_2} S_{S,1} - \frac{Q+Q_i}{V_2} S_{S,2} - \frac{1}{Y_H} P_{2,2} - \frac{1}{Y_H} P_{1,2} \\
\dot{S}_{O,1} =& - \frac{Q+Q_i}{V_1} S_{O,1} + \frac{Q_i}{V_1} S_{O,2} - \frac{1-Y_H}{Y_H} P_{1,1} - (\frac{4.57}{Y_A} + 1) P_{3,1}.
\end{aligned}
\tag{10}
$$

In (10), the subscripts $n = 1, 2$ on the state variables denotes concentrations in compartment $n$. The symbol $P_{m,n}$ means the process rate $m$ in compartment $n$. The notation in (10) is explained in Table 4.1, and the numerical values of the different parameters are given in Appendix A. Note that the symbol $Q_i$ used in (10) can be regarded as the sum of internal recirculation flow rate and the flow rate of recirculated sludge from the clarifier as defined in Figure 1. This does not affect the behaviour of the soluble components, thus the analysis presented in the sequel is not affected. Further, the relevant

process rates in (10) are given by

$$
\begin{aligned}
P_{1,n} &= \mu_H \frac{S_{S,n}}{K_S + S_{S,n}} \frac{S_{O,n}}{K_{O,H} + S_{O,n}} \\
P_{2,n} &= \mu_H \frac{S_{S,n}}{K_S + S_{S,n}} \frac{K_{O,H}}{K_{O,H} + S_{O,n}} \frac{S_{NO,n}}{K_{NO} + S_{NO,n}} \qquad n = 1,\ 2 \\
P_{3,n} &= \mu_A \frac{S_{NH,n}}{K_{NH} + S_{NH,n}} \frac{S_{O,n}}{K_{O,A} + S_{O,n}}.
\end{aligned}
\tag{11}
$$

Table 1: *Nomenclature for the bioreactor models.*

| **Symbol** | **Explanation** |
|---|---|
| $Q$ | Influent flow rate |
| $Q_i$ | Internal recirculation flow rate |
| $V_1$ | Volume of tank 1, the anoxic tank |
| $V_2$ | Volume of tank 2, the aerobic tank |
| $\eta_g$ | Correction factor for anoxic growth of heterotrophs |
| $i_{XB}$ | Quotient between the mass of nitrogen and the mass of the chemical oxygen demand |
| $K_{\mathrm{NH}}$ | Ammonium half saturation constant for autotrophs |
| $K_{\mathrm{NO}}$ | Nitrate half saturation constant for heterotrophs |
| $K_{\mathrm{O},A}$ | Oxygen half saturation constant for autotrophs |
| $K_{\mathrm{O},H}$ | Oxygen half saturation constant for heterotrophs |
| $K_S$ | Half saturation constant for heterotrophs |
| $\mu_A$ | Autotrophic max. specific growth rate |
| $\mu_H$ | Heterotrophic max. specific growth rate |
| $Y_A$ | Autotrophic yield |
| $Y_H$ | Heterotrophic yield |

# 5 Analysis of the Model

In this section, the previously described bioreactor model will be analysed using the RGA and the HIIA described in Section 2 and Section 3. One objective is to investigate the cross couplings in the system and to choose suitable control structures. The desired control structure may change with different operating points since the system is nonlinear. Another objective is to illustrate the performance of both methods, i.e. what different conclusions that can be drawn from each of the methods. For instance, how can the HIIA be used to determine a suitable sparse multivariable control structure, and what can be seen from the RGA in the corresponding case.

## 5.1 Linearisation of the Model

Both the RGA and the HIIA are defined for linear models. In order to perform the analysis, the model (10) needs to be linearised around each operating point. In practise, this was done with the MATLAB function *linmod*. From the linearisation procedure, standard linear state space models of the form

$$\begin{aligned} \Delta\dot{x} &= A\Delta x + B\Delta u \\ \Delta y &= C\Delta x \end{aligned} \tag{12}$$

are obtained. Here $x$ is the state vector

$$x = \begin{bmatrix} S_{NH,1} & S_{NH,2} & S_{NO,1} & S_{NO,2} & S_{S,1} & S_{S,2} & S_{O,1} \end{bmatrix}^T$$

and $u$ is the input signal vector

$$u = \begin{bmatrix} Q_i & S_{S,in} \end{bmatrix}^T. \tag{13}$$

The symbol $\Delta$ refers to deviation from the operating point so that $\Delta x = x - \bar{x}$ and $\Delta u = u - \bar{u}$, where $\bar{u}$ is the constant input signal vector that renders the operating point $\bar{x}$. The output signal vector is $y = [S_{NO,1}\ S_{NO,2}]^T$ and $\Delta y = y - \bar{y}$. The matrix $A$ is a 7×7 matrix, $B$ is a 7×2 matrix and the matrix $C$ is consequently given by

$$C = \begin{bmatrix} 0 & 0 & 1 & 0 & 0 & 0 & 0 \\ 0 & 0 & 0 & 1 & 0 & 0 & 0 \end{bmatrix}$$

independent of the chosen operating point. The corresponding transfer function matrix is then

$$G(s) = C(sI - A)^{-1}B. \tag{14}$$

A first impression of the possible (stationary) cross couplings in the system can be obtained from the steady state operational maps of the nonlinear model. Such operational maps are also used by, for instance, Ingildsen (2002) and Galarza *et al.* (2001) in order to analyse the behaviour of bioreactors. In Figures 2 and 3 the stationary nitrate concentrations of the anoxic and aerobic compartments respectively are plotted against the two input signals $Q_i$ and $S_{S,in}$. From these operational maps it is clear that the system behaves nonlinearly, i.e. the stationary characteristics are different depending on the choice of operating point. For instance, it is seen in Figure 3 that in order to accomplish a change in $S_{NO,2}$ for low values of the input signals, the concentration of readily biodegradable substrate in the influent, $S_{S,in}$ should be used. For larger values of the input signal $S_{S,in}$, the change seems to be best accomplished if the internal recirculation flow rate $Q_i$ is altered. The Figure 2 is more difficult to interpret, it seems that both inputs have an impact on the output over the whole operating range, although the relative importance of the inputs depends on the choice of operating point. A general conclusion that can be drawn is, however, that for high values of the input signal $S_{S,in}$, the gain is low for both the input signals.

Although these plots contains only stationary values for the open loop system and therefore can not be assumed to fully describe all cross couplings in the system, we will use them to roughly validate the results obtained from the linear analysis utilising the RGA and the HIIA.

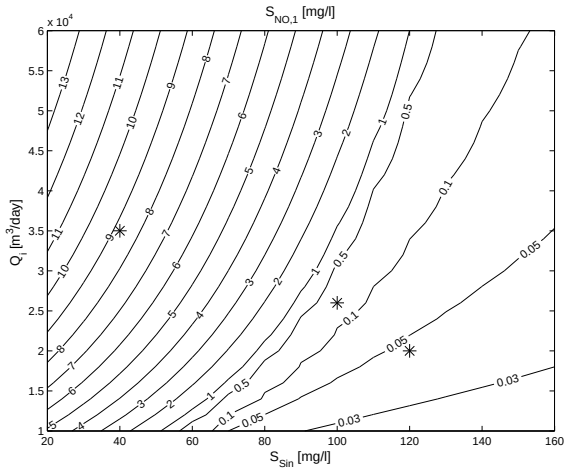


Figure 2: Stationary operational map for the nitrate concentration in the anoxic compartment, $S_{NO,1}$.

As indicated above, Figure 3 implies that there are two different areas in

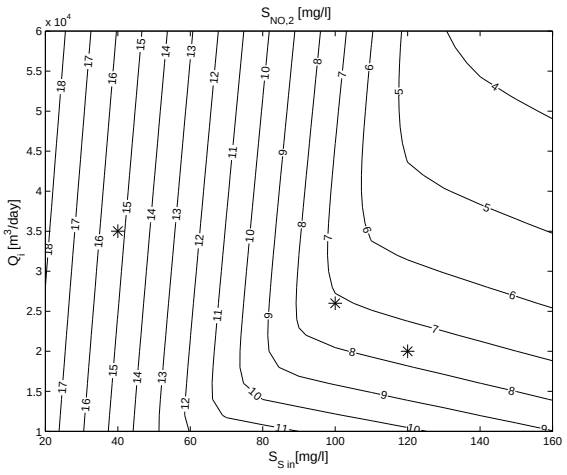


Figure 3: Stationary operational map for the nitrate concentration in the aerobic compartment (effluent water), $S_{NO,2}$.

which the process may show different cross couplings. In order to analyse this behaviour, three different operating points will be considered. The three operating points are marked by stars (* ) in the operational maps in Figure 2 and Figure 3. These are the ones corresponding to the constant input signals given by

$$\begin{aligned} \bar{u}_1 &= \begin{bmatrix} 35000 & 40 \end{bmatrix}^T \\ \bar{u}_2 &= \begin{bmatrix} 26000 & 100 \end{bmatrix}^T \\ \bar{u}_3 &= \begin{bmatrix} 20000 & 120 \end{bmatrix}^T \end{aligned} \tag{15}$$

where the units are $m^3$/day for the first input signal and mg(COD)/l for the other. The first operating point given by $\bar{u}_1$ lies in the area where the second input signal, the concentration of readily biodegradable substrate in the influent water, $S_{S,in}$, is low. The second operating point given by $\bar{u}_2$ lies in the transition phase between the areas, and the third point is in the area where the concentration of readily biodegradable substrate in the influent water is high.

## 5.2 Scaling of the Linearised Model

As mentioned in Section 3, the HIIA is a scaling dependent tool. In order to be able to compare the different elements of the HIIA directly, the linearised model obtained by (12) and (14) must be properly scaled. A standard procedure (as described in for instance Skogestad and Postlethwaite (1996)) for

how to scale a model is to introduce the scaled variables according to

$$u = D_u^{-1} u^o \tag{16a}$$

$$y = D_y^{-1} y^o \tag{16b}$$

where the original model is given by

$$y^0(t) = G^o(p) u^o(t) \tag{17}$$

and the superscript "$^o$" denotes the original (or physical) variables. Thus, $G^o(p)$ denotes the original transfer function matrix between output $y^o(t)$ and input $u^o(t)$; $D_u$ and $D_y$ are diagonal scaling matrices. Thus the transfer function of the scaled model is given by

$$G(s) = D_y^{-1} G^o(s) D_u. \tag{18}$$

There exist many different possibilities for choosing the scaling matrices $D_y$ and $D_u$ depending on what the desired achievements are. In this paper the model is scaled in such a manner that the maximum deviation from the average point of each signal lies in the interval [-1,1]. This is achieved here by choosing

$$D_u = \begin{bmatrix} 60000 & 0 \\ 0 & 160 \end{bmatrix}$$

$$D_y = \begin{bmatrix} 3 & 0 \\ 0 & 3 \end{bmatrix}$$

where the diagonal elements in $D_u$ are the maximum allowed value of the respective input signal and the elements in $D_y$ states that a maximum deviation in the output of three units is accepted. For a more detailed description on the subject of scaling, see for instance Skogestad and Postlethwaite (1996).

## 5.3 RGA Analysis of the Model

To test the ability of the RGA to provide reasonable pairing suggestions, the stationary RGA was calculated for the linearised models for each of the chosen operating points. The results were

$$RGA(G(0))_{\bar{u}_1} = \begin{bmatrix} 1.1979 & -0.1979 \\ -0.1979 & 1.1979 \end{bmatrix} \tag{19}$$

$$RGA(G(0))_{\bar{u}_2} = \begin{bmatrix} 0.3327 & 0.6673 \\ 0.6673 & 0.3327 \end{bmatrix} \tag{20}$$

$$RGA(G(0))_{\bar{u}_3} = \begin{bmatrix} 0.3263 & 0.6737 \\ 0.6737 & 0.3263 \end{bmatrix}. \tag{21}$$

Clearly, since the anti-diagonal elements in the RGA matrix corresponding to the first operating point are negative and the diagonal elements are fairly close to one, the RGA in this case suggests a diagonal controller, i.e. that the first input signal $Q_i$ should be used to control the output $S_{NO,1}$ and the second input, $S_{S,in}$, should control the output $S_{NO,2}$. The latter also seems probable when comparing the results to the operational map in Figure 3, provided that a decentralised control structure is to be used.

For both the other operating points, anti-diagonal control structures are suggested, although without any strong indication since the diagonal element of the RGA matrix is quite far from one in both cases. For the second operating point it is hard to evaluate the validity of this from the operational maps, since the operating point lies in a transition phase. The result for the third operating point, however, seems reasonable when considering the operational maps.

It should once again be stressed that only the stationary RGA has been considered here, and that the RGA only aims to provide the best possible decentralised controller. No conclusions about suitable multivariable control structures can be drawn from the example above.

## 5.4 HIIA Analysis of the model

As mentioned before, the HIIA is a measure that do not require decentralised control, instead it indicates the size of the impact of each input signal on each output signal. It is therefore interesting to compare the results from the HIIA analysis to the results from the RGA analysis. The HIIA as defined in Section 3 was calculated for the linearised and scaled models for each operating point. The obtained results were

$$\Sigma_H^{\bar{u}_1} = \begin{bmatrix} 0.1501 & 0.3552 \\ 0.0474 & 0.4474 \end{bmatrix} \tag{22}$$

$$\Sigma_H^{\bar{u}_2} = \begin{bmatrix} 0.1290 & 0.1332 \\ 0.4131 & 0.3247 \end{bmatrix} \tag{23}$$

$$\Sigma_H^{\bar{u}_3} = \begin{bmatrix} 0.0092 & 0.0051 \\ 0.7557 & 0.2300 \end{bmatrix}. \tag{24}$$

For the first operating point, the HIIA indicates that the first output signal, $S_{NO,1}$, is about equally dependent on both input signals since the elements on the first row in the HIIA matrix have the same magnitude of orders. Further, it can be seen from the second row that the second output, $S_{NO,2}$, mostly depends on the second input signal, $S_{S,in}$. The corresponding HIIA element is also of the the same size as the elements in the first row, while the other element in the second row is considerably smaller. A natural interpretation of the HIIA matrix in this case is therefore that a good option for controlling the process in this operating range may be a sparse multivariable controller taking this into account. A natural control structure selection would therefore be

$$U(s) = \begin{bmatrix} F_1(s) & F_3(s) \\ 0 & F_2(s) \end{bmatrix} E(s) \tag{25}$$

where $F_1(s)$, $F_2(s)$ and $F_3(s)$ are the transfer functions of each sub controller, $U(s)$ is the Laplace transform of the input signal vector as defined in (13) signal and $E(s)$ is the Laplace transform of the control error vector, i.e. a vector containing the control errors of $S_{NO,1}$ and $S_{NO,2}$.

In the second operating point, corresponding to the transition phase between the operating ranges, all elements in the HIIA matrix are of the same magnitude of orders. This indicates that a full multivariable control structure should be chosen here.

Finally, in the third operating point both elements in the first row of the HIIA matrix are small compared to the elements in the second row. This indicates that the first output signal could be difficult to control at all. A physical interpretation of this will be given in Section 7.

Note that no pre-filtering of the transfer functions is performed before

calculating the HIIA. A pre-filtering procedure was evaluated but made no difference in the results and was therefore omitted.

# 6 Control Simulations

In order to illustrate the findings in the previous section, some control experiments were performed. As an example, control of the nonlinear system (10) in the neighbourhood of the first operating point given by the input signal $\bar{u}_1$ in (15) is considered here. Both a decentralised control structure and a simple multivariable strategy are evaluated. The purpose is to compare the results from the linear analysis in the previous section to the actual results obtained when controlling the nonlinear system given by (10).

## 6.1 Decentralised Control

A decentralised control law with the input-output pairing recommended by both the RGA analysis in (19) and the HIIA in (22) was evaluated. The results in (19) and (22) both suggested that if a decentralised control structure was to be used, the natural pairing selection was to control the first output signal, $S_{NO,1}$, by manipulating the first input signal, $Q_i$. Consequently, the second output, $S_{NO,2}$, should be controlled by manipulating the second input signal $S_{S,in}$. Thus, the decentralised control law can be written as

$$Q_i(s) = F_1(s)E_1(s) \tag{26}$$

$$S_{S,in}(s) = F_2(s)E_2(s) \tag{27}$$

where $E_1(s)$ is the Laplace transformed control error of the first loop, i.e. $e_1(t) = S^{sp}_{NO,1}(t) - S_{NO,1}(t)$, and $E_2(s)$ is the Laplace transformed control error of the second loop, i.e. $e_2(t) = S_{NO,2}(t) - S^{sp}_{NO,2}(t)$ since this process is known to have negative gain. Here, $S^{sp}_{NO,1}$ and $S^{sp}_{NO,2}$ denote the set-point values of the output signals respectively.

The controllers $F_1(s)$ and $F_2(s)$ were in this experiment chosen as ordinary PI-controllers and were tuned in order to achieve approximately the same rise time in both control loops to make later comparisons meaningful. The used PI-controllers were

$$F_1(s) = 8000 + \frac{7000}{s} \tag{28}$$

$$F_2(s) = 15 + \frac{8}{s} \tag{29}$$

where the large difference in size between the parameters in the controllers are explained by the large gain differences in the open loop systems.

The decentralised control law (26)-(27) was then used to control the non-linear system (10). Figure 4 shows the output responses of the system when a 10 % step change in the set-point of the first output, $S_{NO,1}^{sp}$, is applied. In the same way, Figure 5 shows the output responses for a 10 % step change in the set-point value of the second output, $S_{NO,2}^{sp}$.

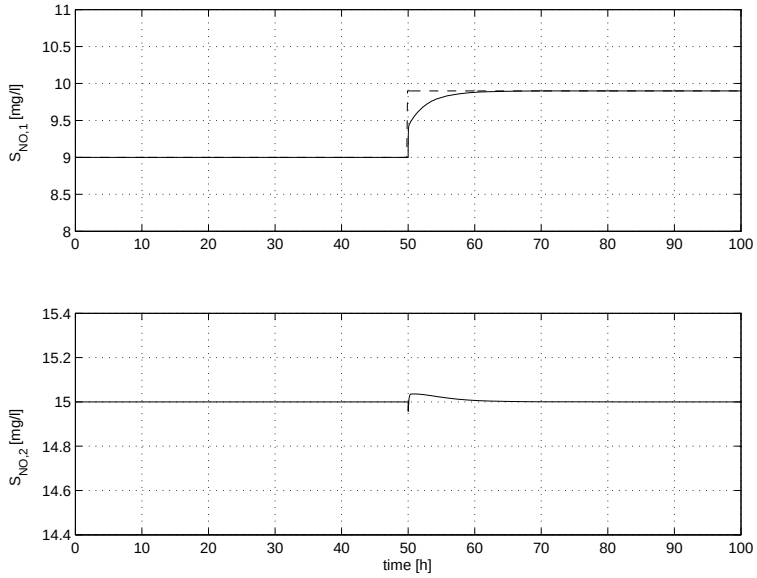


Figure 4: Decentralised control output responses of the system (10) for a step change in the set-point of the first output, $S_{NO,1}$. Upper plot: Solid line shows the response of the output $S_{NO,1}$. Dashed line shows the set-point value. Lower plot: The response of the second output $S_{NO,2}$ is plotted.

The conclusions from the HIIA in (22) were that the first output, $S_{NO,1}$, is affected by both the input signals while the second output $S_{NO,2}$ is mainly affected by the second input signal, $S_{S,in}$. Considering the control law (26)-(27) it is clear by definition that a change in the set-point $S_{NO,1}^{sp}$ causes a direct change in the first input signal, $Q_i$ while the second input signal is unaffected. In the same manner, a change in the other set-point $S_{NO,2}^{sp}$ causes an immediate change in the second input, $S_{S,in}$, but leaves the first input signal unaffected.

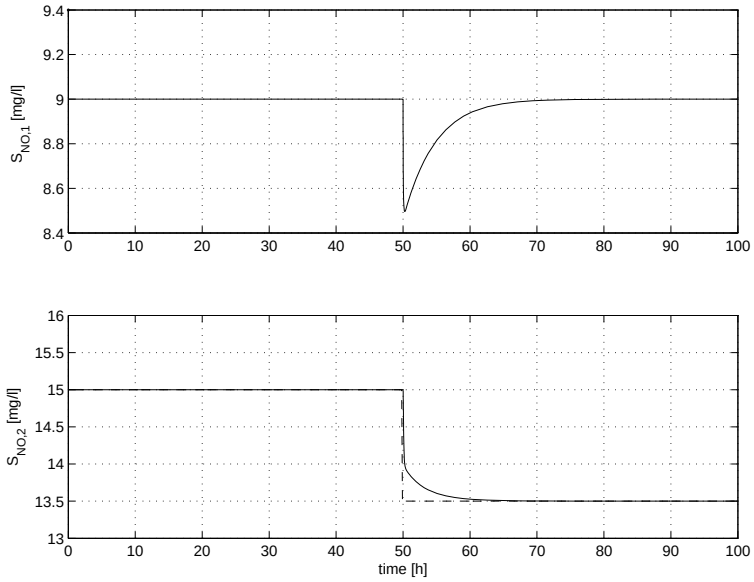


Figure 5: Decentralised control output responses of the system (10) for a step change in the set-point of the second output, $S_{NO,2}$. Upper plot: The response of the first output $S_{NO,1}$ is plotted. Lower plot: Solid line shows the response of the output $S_{NO,2}$. Dashed line shows the set-point value.

Combining this reasoning with the results of the HIIA, it can thus be expected that a step change in $S^{sp}_{NO,1}$ will have a relatively small impact on the output $S_{NO,2}$ while a step change in $S^{sp}_{NO,2}$ will have a larger impact in the first output channel. This is also confirmed by the simulation results in Figures 4 and 5. The disturbance response of the first output is considerably larger when the set-point $S^{sp}_{NO,2}$ is changed than vice versa. It should be noted that like the stationary operational maps, these simulations are merely strong indications that the HIIA in (22) provides a reasonable result. Of course, the performance of the closed loop system depends also on the choice of decentralised controller. However, using reasonable controllers tuned to achieve same rise time in both control loops should make the comparison above relevant.

## 6.2 Multivariable Control

Next, a simple multivariable control strategy is evaluated. The specific structure of the controller is decided using the HIIA analysis results. In Section 5.4, it was concluded from the HIIA analysis that in the neighbourhood of the

first operating point given by the input signal $\bar{u}_1$ in (15), a structured multivariable controller might be preferable to decentralised control. To choose a suitable control structure, first note that according to (22), the dependence of the first input signal on the second output signal is relatively low. One possibility to perform the control design could therefore be to approximate the nonlinear system (10) with a triangular linear system according to

$$\begin{bmatrix} S_{NO,1}(s) \\ S_{NO,2}(s) \end{bmatrix} = \begin{bmatrix} G_1(s) & G_3(s) \\ 0 & G_2(s) \end{bmatrix} \begin{bmatrix} Q_i(s) \\ S_{S,in}(s) \end{bmatrix} \tag{30}$$

where the elements in the transfer function matrix are obtained by linearising the nonlinear system in the neighbourhood of the operating point given by the input signal $\bar{u}_1$.

Since the second output, $S_{NO,2}$, is assumed to depend only on the second input, $S_{S,in}$, it is convenient to choose $S_{S,in}$ according to

$$S_{S,in}(s) = F_2(s)(S_{NO,2}(s) - S^{sp}_{NO,2}(s)). \tag{31}$$

The first output signal, $S_{NO,1}$ is affected by both input signals. A suitable choice might be to take this into account in the control law, for instance by letting

$$Q_i(s) = F_1(s)(S^{sp}_{NO,1}(s) - S_{NO,1}(s)) + F_3(s)S_{S,in}(s) \tag{32}$$

where the latter term can be seen as a feedforward part.

Inserting the control signals (31)-(32) into the expression for the linearised system (30) directly yields

$$S_{NO,1}(s) = \frac{G_1(s)F_1(s)}{1 + G_1(s)F_1(s)} S^{sp}_{NO,1}(s) + \frac{(G_1(s)F_3(s) + G_3(s))}{1 + G_1(s)F_1(s)} S_{S,in}(s) \tag{33}$$

$$S_{NO,2}(s) = \frac{-G_2(s)F_2(s)}{1 - G_2(s)F_2(s)} S^{sp}_{NO,2}(s) \tag{34}$$

and it is seen that the system will be completely decoupled if the feedforward controller $F_3(s)$ can be chosen as

$$F_3(s) = \frac{-G_3(s)}{G_1(s)}. \tag{35}$$

In the simulations, the controller $F_3(s)$ was obtained in the way described above. The nonlinear system (10) was linearised in a neighbourhood corresponding to $\begin{bmatrix} S_{NO,1} & S_{NO,2} \end{bmatrix} = \begin{bmatrix} 9 & 15 \end{bmatrix}$ which corresponds to the input signal

values $u_0 = \begin{bmatrix} 39400 & 43 \end{bmatrix}$. Using (35) on the obtained linear model resulted in this case in a strictly proper linear feedforward controller. The controllers $F_1(s)$ and $F_2(s)$ used in the experiment were the same as before, see (28) and (29). The presented control law was applied on the nonlinear system (10). Figures 6 and 7 show the output responses for step changes in the set-point of each output as in the previous simulations. Comparing Figures 5 and 7 it is seen that the impact of the input signal $S_{S,in}$ on the output signal $S_{NO,1}$ is fairly reduced when the feedforward controller is included, that is, the magnitude of the disturbance response in $S_{NO,1}$ when a step change is applied in the set-point of $S_{NO,2}$ is much lower.

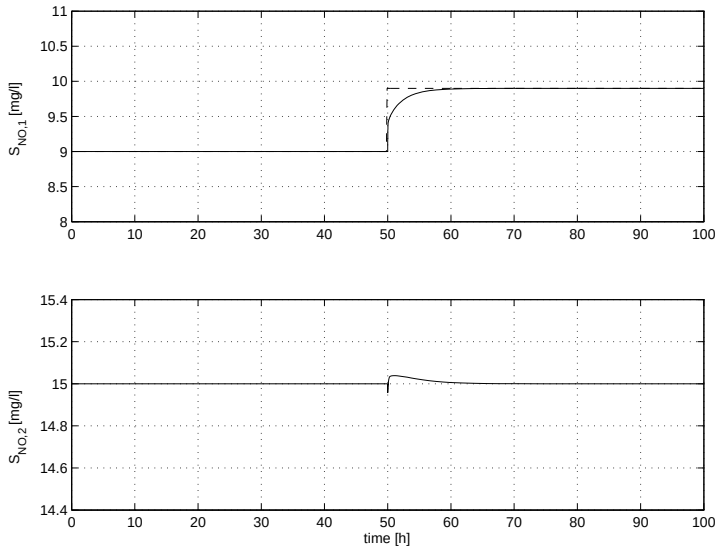


Figure 6: Feedforward control output responses of the system (10) for a step change in the set-point of the first output, $S_{NO,1}$. Upper plot: Solid line shows the response of the output $S_{NO,1}$. Dashed line shows the set-point value. Lower plot: The response of the second output $S_{NO,2}$ is plotted.

In the simulation example considered here, the decoupling above is only approximate since the system is nonlinear. Thus, the disturbance response in the output $S_{NO,1}$ in Figure 7 is not completely attenuated. Further, as mentioned, in the true nonlinear system the impact of the first input signal on the second output is not strictly zero as in the linear model example (30). Therefore, the disturbance response of $S_{NO,2}$ in Figure 6 is not strictly zero. This example, however, shows how the HIIA can be used to determine an approximate decoupling control law for a nonlinear system in the neighbourhood of some operating point.

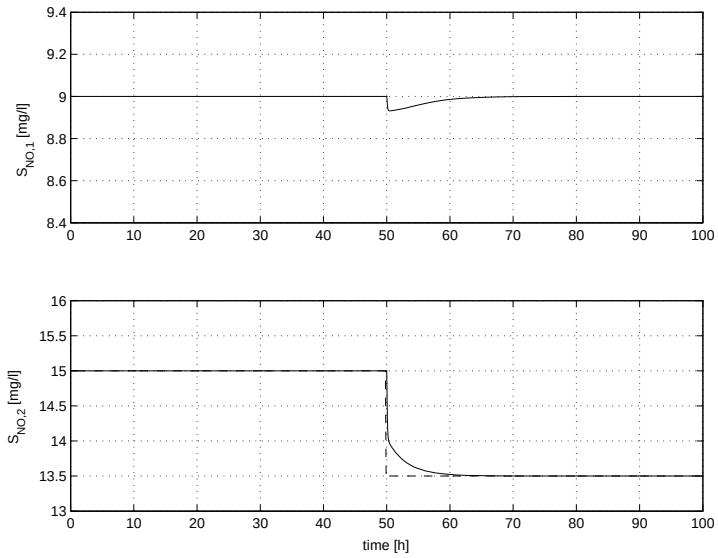


Figure 7: Feedforward control output responses of the system (10) for a step change in the set-point of the second output, $S_{NO,2}$. Upper plot: The response of the first output $S_{NO,1}$ is plotted. Lower plot: Solid line shows the response of the output $S_{NO,2}$. Dashed line shows the set-point value.

# 7 Discussion

Here, the results in the previous section are further discussed. The results from the RGA and the HIIA analysis are also compared to each other and the relevance of the results are discussed from a process knowledge point of view. It should once again be emphasised that the comparison is not entirely fair since the methods in fact investigate different items. The RGA attempts to suggest the best input-output pairing given that a decentralised control structure is to be used. The HIIA uses no such assumption, but gives a measure of how much each input signal affects each output signal. When using the HIIA, one should also bear in mind that the HIIA is dependent of scaling and normalisation which could make the results more difficult to interpret.

For the first operating point, the RGA clearly suggested a diagonal pairing, i.e. the input $Q_i$ (the internal recirculation flow rate) should be used to control the output $S_{NO,1}$ (the nitrate concentration in the anoxic compartment) and that the input $S_{S,in}$ (the concentration of readily biodegradable organic substrate in the influent) should control the output $S_{NO,2}$ (the nitrate concentration in the aerobic compartment). This seems reasonable when considering the operational map in Figure 3 where the stationary value

of $S_{NO,2}$ seem to depend mostly on the stationary value of $S_{S,in}$. From the other operational map in Figure 2 it is harder to draw any conclusions. The HIIA analysis also shows that if a decentralised controller should be used, diagonal pairing is to be preferred. However, the HIIA also provides the information that in this operating point, the output $S_{NO,1}$ is also dependent on the input $S_{S,in}$ and thereby that a sparse multivariable controller according to (25) may be preferable. Thus, the HIIA adds valuable information about the cross couplings in this operating point. The results are also in line with the conclusions that can be drawn from general process knowledge. In the first operating point, $S_{S,in}$ is comparatively low, and there will be a lack of readily biodegradable substrate available for denitrification. Since there is not enough readily biodegradable substrate, the denitrification process in the anoxic compartment will be incomplete, which means that all of the recirculated nitrate is not denitrified. Thus, the nitrate concentration $S_{NO,1}$ will depend both on how much readily biodegradable substrate is added and on how much nitrate is recirculated from the aerobic compartment to the anoxic, i.e. on both input signals. In this situation the nitrate concentration in the aerobic compartment, $S_{NO,2}$, depends mainly on the input $S_{S,in}$, because when the denitrification in the anoxic compartment is incomplete, the internal recirculation only leads to an internal transport of nitrate that does not affect the effluent nitrate concentration of the system. In other words, for low values of $S_{S,in}$, there is no meaning in increasing $Q_i$ since it does not affect the effluent nitrate concentration $S_{NO,2}$. To conclude, both the result from the RGA analysis and from the HIIA analysis therefore seem valid. The HIIA gives more information about the actual cross couplings in the system, and thereby gives an opportunity to design a better controller. The control simulations in Section 6 also confirm these conclusions. Ingildsen (2002) also suggests the particular decentralised control structure suggested by the RGA, however not as a result of a cross coupling analysis but from an economical point of view.

In the second operating point, the RGA gives an indication (however not very strong) that the input-output pairing now should be the reversed, i.e. an anti-diagonal pairing. The conclusion from the HIIA analysis is that a full multivariable controller should be used. It is hard to evaluate the relevance of the RGA analysis from the operational maps or from a physical reasoning. It is clear from the operational maps that in this transition phase, both outputs rely on both inputs, and the HIIA thus seems to provide a reliable result.

In the third operating point, the RGA suggests the same pairing as in the second operating point with approximately the same order of magnitude

on the RGA elements. Here, an interesting difference occur when considering the HIIA analysis. Since the elements on the first row of the HIIA is close to zero, it indicates that the first output $S_{NO,1}$ is difficult to affect at all using any of the two input signals. The second output, $S_{NO,2}$ is mainly affected by the first input signal, $Q_i$, but also to some extent by the other input $S_{S,in}$. A physical interpretation is that in this case the access of readily biodegradable substrate is sufficient, and the concentration $S_{NO,1}$ takes very low values. This means that the denitrification in the anoxic compartment is complete. Since there is a good access to readily biodegradable substrate and the nitrate concentration $S_{NO,1}$ takes low values, $S_{NO,1}$ will not decrease further if more readily biodegradable substrate $S_{S,in}$ is added. If less readily biodegradable substrate is added, $S_{NO,1}$ will not increase as long as the addition is large enough for the denitrification to remain complete. In this operating point, when more nitrate is recirculated through an increase of the internal recirculation flow rate, $Q_i$, $S_{NO,1}$ will not be affected much as long as the transition phase is not passed, i.e. while the denitrification still is complete. If instead the internal recirculation flow rate is decreased, less nitrate has to be denitrified and the stationary $S_{NO,1}$ remains relatively unchanged. Thus, the gains from both input signals are low. As mentioned, the second output, $S_{NO,2}$, is in this operating point mainly affected by the internal recirculation flow rate, $Q_i$. If, for instance, more nitrate is recirculated more nitrate will also be denitrified and the nitrate concentration $S_{NO,2}$ is thus reduced. This behaviour is at least mirrored in the HIIA, although these conclusions are hard to draw directly from the HIIA without any prior process knowledge. In order to control the system in this operating range, i.e. so that a low effluent nitrate concentration is obtained, one possible strategy is to add sufficient amounts of readily biodegradable substrate to achieve complete denitrification in the anoxic compartment. The nitrate concentration in the aerobic compartment can then be moderated by adjusting the internal recirculation flow rate. Expressed in control terminology, the input $S_{S,in}$ should be used to keep the output $S_{NO,1}$ at a low set-point. The input $Q_i$ should be used to control the output $S_{NO,2}$ to some desired value. This specific pairing is also what the RGA recommends, although as seen above, additional useful information can be extracted from the HIIA.

It should be noted that in reality, it might be sufficient to run the process only in the operating range described by the first operating point depending on the actual demands on effluent nitrate concentration. In the overall consideration, process economy should also be weighted into the choice of control structure and desired operating range, not just the goal to reduce nitrate concentration as much as possible. In a case where the process may run

in different operating ranges, however, the use of different control structures in the different operating ranges may provide better control of the process.

# 8 Conclusions

In this paper, the cross couplings in a bioreactor model describing a predenitrifying wastewater treatment plant have been studied. Two different tools were used to evaluate the cross couplings, the Relative Gain Array (RGA) and the Hankel Interaction Index Array (HIIA). The general conclusion from the presented analysis is that both the RGA and the HIIA gives reasonable results for the studied example. The HIIA, however, provides information that the RGA does not. The results from the HIIA analysis can be useful for understanding the actual cross couplings in the system, and are thereby useful for suggesting suitable multivariable control structures. The validity of the results is also illustrated by means of some control experiments. It is also shown how the HIIA can be used in order to determine a suitable multivariable controller structure.

# A Parameter values

Table 2 shows the parameter values that were used in the analysis of the model described by equations (10).

Table 2: *Parameter values used in the model (10)*

| **Parameter** | **Value** | **Unit** | **Comment** |
|---|---|---|---|
| $S_{\mathrm{NH}_i}$ | 31.56 | g N $m^{-3}$ | Influent ammonium conc. |
| $Q$ | 18446 | $m^3$ $day^{-1}$ | |
| $V_1$ | 2000 | $m^3$ | Volume of anoxic reactor |
| $V_2$ | 3999 | $m^3$ | Volume of aerobic reactor |
| $\eta_g$ | 0.8 | - | |
| $i_{XB}$ | 0.08 | - | |
| $K_{\mathrm{NH}}$ | 1.0 | g $NH_3$-N $m^{-3}$ | |
| $K_{\mathrm{NO}}$ | 0.5 | g $NO_3$-N $m^{-3}$ | |
| $K_{\mathrm{O},A}$ | 0.4 | g $O_2$ $m^{-3}$ | |
| $K_{\mathrm{O},H}$ | 0.2 | g $O_2$ $m^{-3}$ | |
| $K_S$ | 10.0 | g COD $m^{-3}$ | |
| $\mu_A$ | 0.5 | $day^{-1}$ | |
| $\mu_H$ | 4.0 | $day^{-1}$ | |
| $X_{B,A}$ | 150 | g COD $m^{-3}$ | |
| $X_{B,H}$ | 2500 | g COD $m^{-3}$ | |
| $Y_A$ | 0.24 | - | |
| $Y_H$ | 0.67 | - | |

# References


Birk, W. (2002). Industry Application of Multivariable Control. PhD thesis. Luleå University of Technology. Luleå, Sweden.

Bristol, E. H. (1966). On a new measure of interaction for multivariable process control. *IEEE Trans. Automatic Control* **AC-11**, 133–134.

Carlsson, B. and A. Rehnström (2002). Control of an activated sludge process with nitrogen removal - a benchmark study. *Water Science and Technology* **45**(4–5), 135–142.

Chien, J., J.S. Freudenberg and C. N. Nett (1992). On relative gain array and condition number. In: *Proceedings of the 31st Conference on Decision and Control*. Tuscon, Arizona, USA. pp. 219–224.

Conley, A. and M. E. Salgado (2000). Gramian based interaction measure. In: *Proceedings of the 39th IEEE Conference on Decision and Control*. Sydney, Australia. pp. 5020–5022.

Galarza, A., E. Ayesa, M. T. Linaza, A. Rivas and A. Salterain (2001). Application of mathematical tools to improve the design and operation of activated sludge plants. Case study: The new WWTP of Galindo-Bilbao, part ii: Operational strategies and automatic controllers. *Water Science and Technology* **43**(7), 167–174.

Häggblom, K. E. (1997). Control structure analysis by partial relative gains. In: *Proceedings of the 36th Conference on Decision and Control*. San Diego, California, USA. pp. 2623–2624.

Halvarsson, B. (2003). Applications of coupling analysis on bioreactor models. Master's thesis. Uppsala University. Uppsala, Sweden.

Henze, M., C. P. L. Grady Jr., W. Gujer, G. v. R. Marais and T. Matsuo (1987). Activated sludge model no. 1. Scientific and Technical Report No. 1. IAWPRC, London.

Henze, M., P. Harremoës, J. la Cour Jansen and E. Arvin (1995). *Wastewater treatment, biological and chemical processes*. Springer-Verlag, Berlin Heidelberg, Germany.

Ingildsen, P. (2002). Realising Full-Scale Control in Wastewater Treatment Systems Using In Situ Nutrient Sensors. PhD thesis. Lund University, Sweden.

Ingildsen, P., G. Olsson and Z. Yuan (2002). A hedging point strategy – balancing effluent quality, economy and robustness in the control of wastewater treatment plants. *Water Science and Technology* **45**(4–5), 317–324.

Jeppsson, U., J. Alex, M. N. Pons, H. Spanjers and P. A. Vanrolleghem (2001). Status and future trends of ICA in wastewater treatment - a european perspective.. In: *Proceedings of the 1st IWA Conference on Instrumentation, Control and Automation*. Malmö, Sweden. pp. 687–694.

Kinnaert, M. (1995). Interaction measures and pairing of controlled and manipulated variables for multiple-input multiple-output systems: A survey. *Journal A* **36**(4), 15–23.

Mc Avoy, T., Y. Arkun, R. Chen, D. Robinson and P. D. Schnelle (2003). A new approach to defining a dynamic relative gain. *Control Engineering Practice* **11**(8), 907–914.

Olsson, G. and B. Newell (1999). *Wastewater Treatment Systems*. IWA Publishing.

Schmidt, H. and E. W. Jacobsen (2003). Selecting control configurations for performance with independent design. *Computers & Chemical Engineering* **27**(1), 101–109.

Skogestad, S. and I. Postlethwaite (1996). *Multivariable Feedback Control*. John Wiley & Sons. Chichester, UK.

Vanrolleghem, P. A. and S. Gillot (2002). Robustness and economic measures as control benchmark performance criteria. *Water Science and Technology* **45**(4–5), 117–126.

Wittenmark, B. and M. E. Salgado (2002). Hankel-norm based interaction measure for input-output pairing. In: *Proc. of the 2002 IFAC World Congress*. Barcelona, Spain.

Wittenmark, B., K. J. Åström and S. B. Jörgensen (1995). *Process Control*. Dep of Automatic Control, Lund University, Lund, Sweden.

Yuan, Z., A. Oehmen and P. Ingildsen (2002). Control of nitrate recirculation flow in predenitrification systems. *Water Science and Technology* **45**(4–5), 317–324.